Astron. Astrophys. 342, 610–613 (1999)

ASTRONOMY AND ASTROPHYSICS

Selected Fe II lifetimes and f-values suitable for a solar abundance study

R. Schnabel[1], **M. Kock**[1], **and H. Holweger**[2]

[1] Institut für Atom- und Molekülphysik, Abteilung Plasmaphysik, Universität Hannover, Callinstrasse 38, D-30167 Hannover, Germany (e-mail: kock@pmp.uni-hannover.de)
[2] Institut für Theoretische Physik und Astrophysik, Universität Kiel, D-24098 Kiel, Germany (e-mail: supas059@astrophysik.uni-kiel.de)

Received 12 October 1998 / Accepted 12 November 1998

Abstract. A selected number of Fe II level lifetimes have been measured anew with an improved experimental equipment and evaluation procedure yielding data with uncertainties around 1%. The lifetimes have been used to rescale the corresponding oscillator strengths and to derive solar abundances. On average, the iron abundance, log N(Fe) = 7.42 ± 0.09 on the scale log N(H) = 12, is further reduced supporting the lower abundance results in the literature.

Key words: atomic data – methods: laboratory – Sun: abundances

1. Introduction

A few years ago we published a small set of Fe II f–values of lines of astrophysical interest (Heise & Kock 1990) giving a solar iron abundance of log N(Fe) = 7.48 ± 0.09 (Holweger et al., 1990). Later Hannaford et al.(1992) measured the corresponding lifetimes anew which they combined with our branching ratios. They obtained a solar abundance of log N(Fe) = 7.48 ± 0.04, in agreement with our result. On the other hand the high Oxford value of Blackwell et al. (1984) derived from Fe I lines, log N(Fe) = 7.67 ± 0.03, is still under discussion. A contribution in solving this puzzle could be better lifetime measurements, especially, by reducing systematic error sources.

We developed an improved apparatus to measure lifetimes below 5 ns more accurately with the time-resolved laser-induced fluorescence (TRLIF) technique. The improvement includes a short laser pulse, a linear ion trap, a faster photodetector and a more sophisticated evaluation procedure. The apparatus has successfully been tested on W II and is now used to measure a selected number of Fe II levels. We present the results together with our rescaled f–values, and also a new abundance determination is given.

2. Experimental

In our TRLIF experiment we use a modified version of our high-current hollow cathode as a sputtering source for iron atoms and ions and a linear Paul trap for storing the ions (see Fig. 1). The cylindrical cathode insert of 35 mm length and a central bore of 6 mm is stopped down to a 0.3 mm aperture on the low-pressure side. Within the discharge the buffer gas pressure is typically 300 Pa so that the trap is filled continuously through the aperture by pressure gradient. While the neutrals move through the trap as an effusive beam the iron ions are trapped in an oval ion cloud with a diameter of a few millimeters. For obtaining an efficient ion trapping the low–pressure side is filled with 3–40 Pa neon as a cooling gas. A more detailed description is given in Schultz-Johanning et al.(1998).

A Quanta Ray DCR 11–3 Nd:YAG laser–pumped dye laser (Lambda Physik: LPD 3002) produces laser pulses of 4–5 ns duration (FWHM) with a spectral bandwidth of 0.2 cm^{-1} and a repetition rate of 10 Hz. The spectral range 220–270 nm is obtained by frequency doubling with a BBO crystal leading to a pulse duration of 3–4 ns. The laser beam is crossed with the ion cloud/beam in the Paul trap. Perpendicular to the laser beam the fluorescence photons are imaged by a lens system onto the photocathode of a multiplier using the magic angle arrangement. We need no longer optical filters for excluding unwanted light because scattered laser light is sufficiently suppressed by a stack of diaphragms, and light from the discharge itself is excluded by the 0.3 mm aperture. Our multiplier (Hamamatsu R2496) has a finite risetime of 700 ps and a non–ideal response function with ringing due to the electrical circuitry. The ringing cannot be smoothed without a loss in time–resolution. We therefore measure the response function separately and include it in our evaluation procedure, see also Engelke et al. (1993) and Schnabel et al. (1995). In addition, we measure the temporal shape of our laser pulse by means of a fast photodiode (Hamamatsu R1328U–52) having a risetime of 60 ps. This arrangement is also used to trigger the fluorescence signal. Moreover, the shape of the laser pulse enters our evaluation procedure. The fluorescence curves are recorded time–resolved by means of a fast digitizing oscilloscope (Tektronix TDS 680 B) with an analog bandwidth of 1 GHz and a realtime scanning rate of 2 × 5 Gigasamples. This instrument allows the record of a full decay curve and simultaneously the record of the temporal laser pulse with a 200 ps time increment which is comparable with the risetime of the oscilloscope. In the present experiment we typically added

Send offprint requests to: M. Kock

Table 1. Fe II radiative lifetimes

Level	Energy (cm^{-1})	Transitions $\lambda_{exc.}$ (nm)			Lifetimes (ns) Ref. [1]	Ref. [2]	Ref. [3]	**this work**
$^6D^o_{7/2}$	38660.04	258.5876	261.1874	263.1324	3.68 ± 0.07		3.75 ± 0.2	**3.64 ± 0.09**
$^6D^o_{5/2}$	38858.96	259.8370	261.7618	263.1048	3.63 ± 0.08		3.7 ± 0.2	**3.70 ± 0.05**
$^6D^o_{3/2}$	39013.21	260.7088	262.0409	262.8294	3.83 ± 0.10		3.7 ± 0.2	**3.73 ± 0.07**
$^4D^o_{7/2}$	44446.88	224.9180				3.02 ± 0.07	3.1 ± 0.2	**2.97 ± 0.02**
$^4D^o_{5/2}$	44784.76	225.1556	226.5995			3.10 ± 0.08	3.1 ± 0.2	**2.90 ± 0.06**
$^4D^o_{3/2}$	45044.17	226.2688					3.0 ± 0.2	**2.91 ± 0.09**
$^4F^o_{5/2}$	45079.88	225.0936	226.0860			3.75 ± 0.14	3.7 ± 0.2	**3.55 ± 0.08**

[1] Biemont et al. (1991), [2] Guo et al. (1992) and [3] Hannaford et al. (1992)

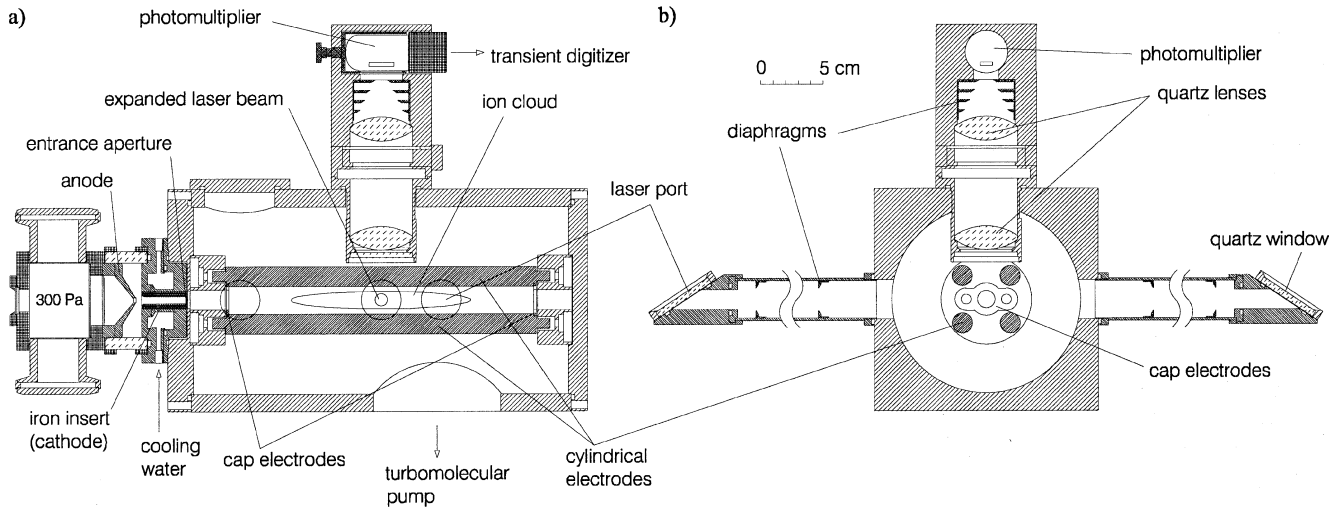

Fig. 1a and b. LIF Apparatus. **a** Cross–sectional view of the linear Paul trap flanged to the hollow cathode. The fluorescence photons are imaged perpendicular to the laser beam onto a photomultiplier tube. Three laser ports can be seen. **b** View from the front of the apparatus.

500 single shots for obtaining a flawless S/N ratio. It is worth mentioning that the measuring time is less than one minute.

3. Lifetime measurements

Evaluation of our LIF signals is done by fitting an exponential decay curve which is convoluted with the response function of our photomultiplier. By this procedure the whole LIF signal can be evaluated including the rising portion. The procedure is described in Engelke et al. (1993). Additionally, we extended the procedure to handle saturation in the fluorescence signals by solving an appropriate rate equation system. Fig. 2 demonstrates the excellent matching between measuring points and fitted curve even if the lifetime is slightly shorter than the FWHM of the laser pulse. During pumping with the laser pulse saturation occurs and also overpumping into third levels. Both transmute the temporal shape of the LIF signal, see also the results of van Lessen et al. (1998). In Fig. 3 a comparison of a fit including saturation with a fit neglecting saturation is given.

In Table 1 seven Fe II level lifetimes are listed together with literature data. Quoted uncertainties refer to the standard deviation of the mean. On each level we made at least 5 inde-

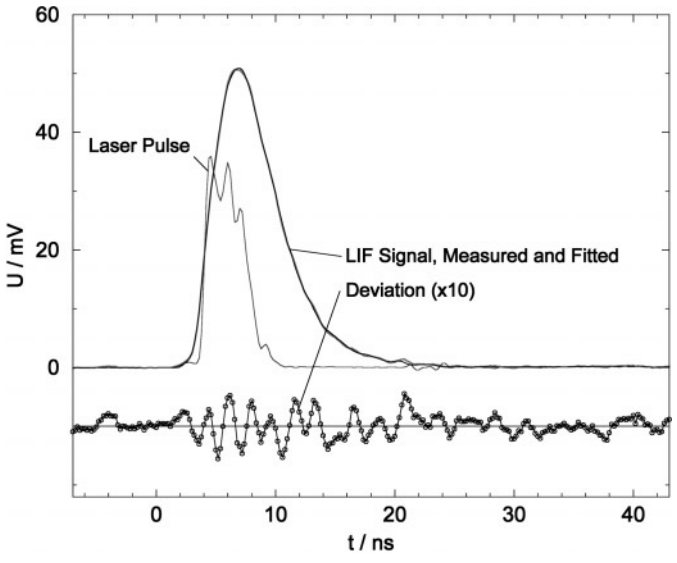

Fig. 2. Time-resolved LIF signal on the Fe II $^4D^o_{7/2}$ level, measured and fitted, together with the exciting laser pulse. The fitted curve matches the measuring points in an excellent way, giving a lifetime of τ = 2.97 ns.

Table 2. Solar iron abundance

Upper Level Energy E_k / Lifetime	λ (nm)	Lower Level	E_i (cm^{-1})	A_{ki} ($10^4\ s^{-1}$)	Δ %	log(gf)	W (mÅ)	**log N(Fe)**
z $^6D^o_{7/2}$ 38660.04 cm^{-1}	325.589	a $^4D_{7/2}$	7955.30	27.7	10	-2.46[a]		
3.64(9) ns	651.607	a $^6S_{5/2}$	23317.60	0.83	12	-3.38	57.6	**7.552**
z $^6D^o_{5/2}$ 38858.96 cm^{-1}	328.130	a $^4D_{5/2}$	8391.94	23.3	10	-2.65[a]		
3.70(5) ns	643.267	a $^6S_{5/2}$	23317.60	0.85	14	-3.51	44.2	**7.419**
z $^4D^o_{7/2}$ 44446.88 cm^{-1}	423.316	b $^4P_{5/2}$	20830.58	71.0	15	-1.81[a]		
2.97(2) ns	462.051	b $^4G_{7/2}$	22810.33	2.49	16	-3.19	56.5	**7.420**
	541.408	a $^4P_{5/2}$	25981.65	0.92	18	-3.48	29.8	**7.424**
	552.513	b $^2H_{9/2}$	26352.80	0.31	20	-3.94	13.1	**7.429**
	771.173	b $^4D_{7/2}$	31483.20	4.86	17	-2.45	49.5	**7.332**[b]
z $^4D^o_{5/2}$ 44784.76 cm^{-1}	435.177	b $^4P_{3/2}$	21812.06	50.8	15	-2.06[a]		
2.90(6) ns	457.633	b $^4F_{5/2}$	22939.35	6.73	18	-2.90	67.0	**7.380**
	465.697	a $^6S_{5/2}$	23317.60	1.43	19	-3.57	33.7	**7.338**
	744.934	b $^4D_{3/2}$	31364.47	1.77	21	-3.06	19.2	**7.252**[b]
	751.583	b $^4D_{7/2}$	31483.18	0.85	22	-3.37	15.1	**7.434**[b]
z $^4D^o_{3/2}$ 45044.17 cm^{-1}	321.045	a $^4P_{5/2}$	13904.82	363	10	-1.65[a]		
2.91(9) ns	526.479	a $^4G_{5/2}$	26055.40	3.52	12	-3.23	48.0	**7.585**
z $^4F^o_{5/2}$ 45079.88 cm^{-1}	316.309	a $^4P_{5/2}$	13474.41	19.2	15	-2.77[a]		
3.55(8) ns	523.462	a $^4G_{7/2}$	25981.65	24.8	18	-2.22	88.3	**7.366**
	562.749	a $^2F_{7/2}$	27314.93	0.29	17	-4.09	7.5	**7.397**

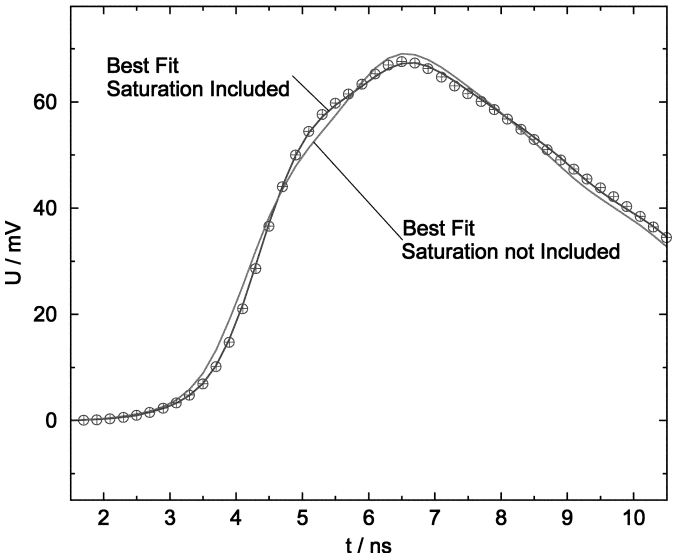

Fig. 3. Measuring points of a TRLIF signal and fitted curves. If saturation is included the fit matches the data points in an excellent way.

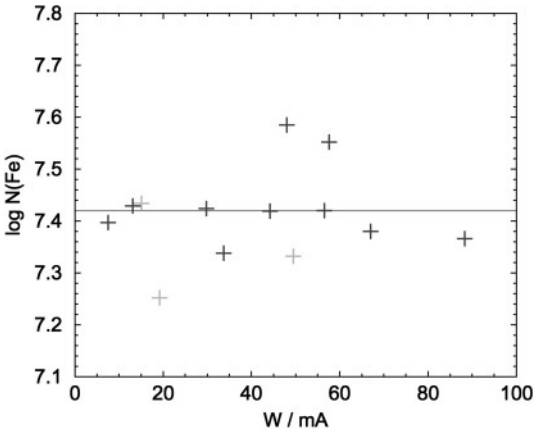

Fig. 4. Solar iron abundance versus equivalent width

pendent measurements on up to three transitions using differing buffer gas conditions and laser pulse energies. There is consistency within the mutual error bars, although the measuring procedures are quite different. On the other hand our lifetimes are shorter than the values we used in Kroll & Kock (1987). Therefore we can rescale the absolute transition probabilities presented in Heise & Kock (1990) where we used a reference line from Kroll & Kock.

4. Solar iron abundance

In Table 2 our log(gf) values, equivalent widths and iron abundance data are listed. The log(gf) values are taken from Heise & Kock (1990) but rescaled with our new lifetime data. The reference lines marked with [a] are also rescaled. Following our former model-atmosphere analysis our new abundance values become slightly lower than in Holweger et al. (1990), because of the enlarged log(gf) values. The final solar iron abundance resulting from the entire sample of Fe II lines becomes

$$\log \mathrm{N(Fe)} = 7.42 \pm 0.09$$

on the usual scale with log N(H)=12. Following Holweger et al. (1990) the three infrared lines marked with [b] are half weighted. The quoted uncertainty refer to the internal accuracy, i.e. the standard deviation of the individual lines. This corresponds to a standard deviation of the mean of less than 0.05 dex which is also quoted in Hannaford et al. (1992). The difference to their result of 7.48 $\pm$ 0.04 is a consequence of different f–values (-0.007 dex), equivalent widths (-0.005 dex), Van-der-Waals-broadening (-0.017 dex) and a different weighting of the individual lines.

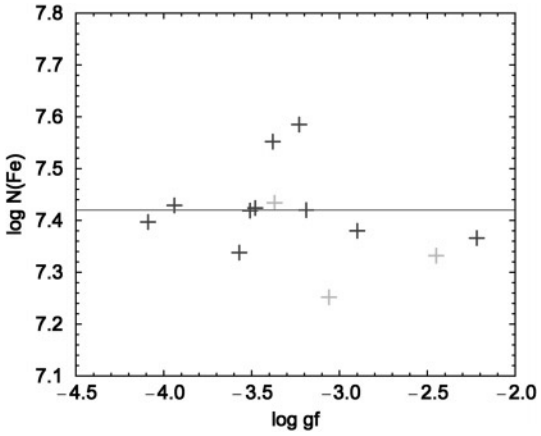

Fig. 5. Solar iron abundance versus log(gf) value

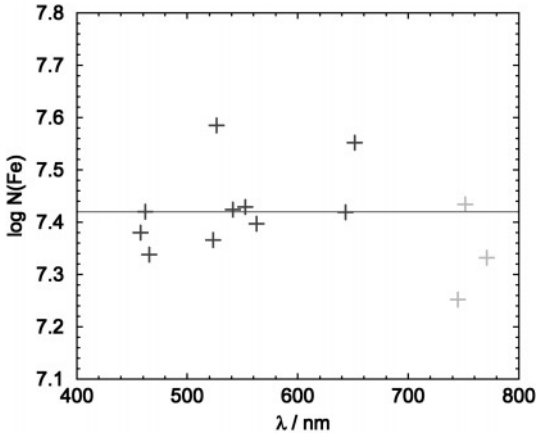

Fig. 6. Solar iron abundance versus wavelength

As shown in Figs. 4, 5 and 6 no significant dependence of abundance on equivalent width, log(gf) value and wavelength exists, with the possible exception of the three infrared lines (shown as thin crosses). It is a remarkable outcome of the present paper that the solar iron abundance has shifted to a still lower value compared to that of Blackwell et al. (1984).

References

Biemont E., Baudoux M., Kurucz R.L., Ansbacher W., Pinnington E.H., 1991, A&A 249, 539
Blackwell D.E., Booth A.J., Petford A.D., 1984, A&A 132, 236
Engelke D., Bard A., Kock M., 1993, Z. Phys. D 27, 325
Guo B., Ansbacher W., Pinnington E.H., Ji Q., Berends R.W., 1992, Phys. Rev. A 46, 641
Hannaford P., Lowe R.M., Grevesse N., Noels A., 1992, A&A 259, 301
Heise C., Kock M., 1990, A&A 230, 244
Holweger H., Heise C., Kock M., 1990, A&A 232, 510 A., 1992, A&A 259, 301
Kroll S., Kock M., 1987, A&A 67, 225
Lessen M. van, Schnabel R., Kock M., 1998, J. Phys., B: At. Mol. Opt. Phys. 31, 1931
Schnabel R., Bard A., Kock M., 1995, Z. Phys. D 34, 223
Schnabel R., Schultz-Johanning M., Kock M., 1998, EPJ D 4(3), 267
Schultz-Johanning M., Schnabel R., Kock M., 1998, EPJ D, in press